J Intell Robot Syst (2018) 89:87–106
DOI 10.1007/s10846-017-0563-0

The Target Differential Game with Two Defenders

David W. Casbeer · Eloy Garcia · Meir Pachter

Received: 9 June 2016 / Accepted: 25 April 2017 / Published online: 4 May 2017

Abstract A cooperative aircraft differential game where an Attacker missile pursues an unmanned aerial vehicle (UAV) herein called the Target is addressed. The Target UAV cooperates with up to two Defender missiles which are launched in order to intercept the Attacker before the latter reaches the Target. This is a scenario with important military applications where each one of the agents is an autonomous air vehicle. Each agent plans and corrects its course of action in order to defeat an opposing force while simultaneously optimizing an operational relevant cost/payoff performance measure. The Target and the Defenders cooperate to form a team against the Attacker. The results in this paper build on the solution of a three agent differential game, where the three players are the Target, the Attacker, and one Defender; in this paper, the benefits of firing a second Defender are considered. Indeed, launching two interceptor missiles is a standard procedure by providing redundant backup. Building on the solution of the one-Defender problem, it is possible to address a seemingly intractable problem, where the Target needs to decide which Defender(s) to cooperate with, in addition to obtaining the optimal headings of every player in the game. Given the initial positions of the players, we solve the problem of determining if a second Defender improves the Target/Defender(s) payoff and provide the optimal strategies for each of the agents involved. Finally, we address the game of kind (for the case of one Defender) which provides the safety regions to determine which side will win based on the initial state. These safety regions provides the Target's area of vulnerability, and using these results, we describe the reduction to the Target's vulnerability area brought by an additional Defender.

Keywords Autonomous air vehicles · Differential games · Missile guidance

D. W. Casbeer (✉) · E. Garcia
Control Science Center of Excellence, Air Force Research Laboratory, Wright-Patterson AFB, OH 45433, USA
e-mail: david.casbeer@us.af.mil

E. Garcia
e-mail: eloy.garcia.2@us.af.mil

M. Pachter
Department of Electrical Engineering, Air Force Institute of Technology, Wright-Patterson AFB, OH 45433, USA
e-mail: meir.pachter@afit.edu

1 Introduction

The Active Target Defense Differential Game (ATDDG) represents an important and practical multi-agent pursuit-evasion dynamic game. The ATDDG in [15] is modeled as a three-agent zero-sum pursuit-evasion differential game. A two-agent team is formed which consists of a Target and a Defender, who cooperate, and the Attacker is the opposition. The goal of the Attacker is to come as close as possible to the

Target, possibly capturing the Target. The Target cooperates with the Defender, who is trying to intercept the Attacker as far away from the Target as possible, before the latter captures the Target. It is assumed that the agents/air vehicles have simple motion kinematics á la Isaacs [14]. It is also assumed that the Attacker is aware of the Defender's position, so that full state information is available.

The ATDDG falls into the realm of pursuit-evasion scenarios involving multiple agents, which have been considered by different authors in the context of dynamic games [6, 13, 17]. To help analyze this complex situation, [1] and [13] utilize a dynamic Voronoi diagram to investigate scenarios with several pursuers aiming to capture an evader within a bounded domain. In [4], a multi-agent scenario is considered where a number of pursuers are assigned to intercept a group of evaders and where the goals of the evaders are assumed to be known. Cooperation between two agents with the goal of evading a single pursuer has been addressed in [5]. Scott and Leonard [25] investigated a bio inspired scenario where two evaders coordinate their strategies to evade a single pursuer, but at the same time keep them close to each other.

Recently, the active aircraft defense scenario involving the Target, the Attacker, and the Defender has received increased attention. A number of authors have proposed different guidance laws for the Attacker and Defender. Ref. [19] addressed the case where the Defender implements Command to the Line of Sight guidance to pursue the Attacker, which requires the Defender to have at least the same speed as the Attacker. Rubinsky and Gutman [21, 22] presented an analysis of the end-game Target-Attacker-Defender (TAD) scenario based on the Attacker/Target miss distance for *a non-cooperative* Target and Defender duo. A different guidance law for the TAD scenario was given by Yamasaki et.al. [28, 29]. These authors investigated a guidance method they called Triangle Guidance, where the objective is to command the defending missile to be on the line-of-sight between the attacking missile and the aircraft for all time while the aircraft follows some predetermined trajectory. The approach used in this paper is different than the references cited above in the sense that strict cooperation between the Target and the Defender is imposed in order to achieve the two objectives: intercept the Attacker and maximize the terminal Target-Attacker separation.

Different variations of the TAD problem, which take into account different types of cooperation have been proposed. In [23, 24] optimal controls (lateral acceleration for each agent including the Attacker) are provided for the case of an aggressive Defender, that is, it is assumed that the Defender has a maneuverability advantage. A linear quadratic optimal control problem is posed where the Defender's control effort weight is driven to zero to model its aggressiveness. The work [20] provided a game theoretical analysis of the TAD problem using different guidance laws for both the Attacker and the Defender. The cooperative strategies in [27] allow for a maneuverability disadvantage for the Defender with respect to the Attacker. Shaferman and Shima [26] implemented a Multiple Model Adaptive Estimator to identify the guidance law and parameters of the incoming missile and optimize the Defender's strategy to minimize its control effort. The authors of [18] analyze different types of cooperation assuming the Attacker is oblivious of the Defender and its guidance law is known. Two different one-way cooperation strategies were discussed: when the Defender acts independently, the Target knows its future behavior and cooperates with the Defender, and vice versa. Two-way cooperation where both Target and Defender communicate continuously to exchange their states and controls is also addressed, and this strategy is shown to have better performance than the one-way models of cooperation - as expected. The advantages of Target/Defender cooperation were also highlighted by [16] where the TAD problem is formulated as linear quadratic differential game. In this reference the Target helps the Defender to minimize the miss distance of interception of the Attacker.

In [11, 12], the authors considered the TAD scenario where the Attacker employs a fixed guidance law. The Target and Defender cooperate in order to intercept the Attacker and maximize the terminal separation between the Target and the Attacker. Because the Attacker guidance is fixed, the Target/Defender team solves a cooperative optimal control problem to determine their best strategies to defeat the Attacker.

The active target defense scenario is formulated as a zero-sum differential game with perfect (state) information in [9] and [15]. Having assumed that the Attacker's situational awareness is such that it also knows the instantaneous position of the Defender, this strategy provides better performance for the Attacker than when it uses the conventional Pure Pursuit (PP)

or Proportional Navigation (PN) guidance laws. For a cooperative Target/Defender team, we showed in [9] that if the Attacker wishes to minimize the final separation between the Target's terminal position and the point where the Attacker is intercepted by the Defender then the standard guidance laws do *not* achieve this goal. A comparison between the pursuit strategies PP, PN, and the solution to the differential game shows that the PP and PN guidance laws return a terminal distance that is greater than that provided by the solution of the ATDDG. Hence, an "intelligent" Attacker will be rewarded by implementing the optimal policy obtained by solving the ATDDG. The joint objectives of intercepting the Attacker and maximizing the terminal Target-Attacker separation provide an improved level of safety for the valuable Target asset.

In this paper we consider the following novel problems. First, for given Target and Attacker positions and given the locations of two potential Defenders (two friendly UAVs ready to fire one Defender missile each) we need to determine if there is a benefit to the Target if both missiles are fired. In other words, determine if the final separation between the Target and the point where the Attacker will be intercepted by either or both Defenders will be increased with respect to the solutions of the individual ATDDG. Second, when both Defenders are fired, determine the solution of the two-defender ATDDG. This solution should provide the optimal headings of the Target, the Attacker, and both Defenders such that the Target/Defenders team maximizes and the Attacker minimizes the terminal Target-Attacker distance. The consideration of a differential game where the Target cooperates with two Defenders represents a new scenario which has not been addressed before in existing literature.

Preliminary results concerning the ATDDG with two Defenders were presented in [3]. The present paper extends and complements [3] by providing the solution to the game of kind for the one Defender case as a function of the Target/Defender separation. We provide a closed-form solution that determines the winning regions of each team. The winning region of the Attacker corresponds to the area of vulnerability of the Target. Based on the proposed solution of the game of kind for the one Defender case, we analyze the advantages (as measured by the reduction of the Target's area of vulnerability) of the two Defender ATDDG compared to the one Defender case. Another extension is given by the novel root locus analysis of the polynomial equation that provides the optimal interception point. This analysis is useful in order to determine the properties of the ATDDG solution and it implementation in the one Defender and in the two Defender cases.

Overall, the ATDDG represents a challenging problem with significant military applications involving autonomous air vehicles (the Target UAV and the Attacker and Defender missiles). Each team/agent needs to autonomously decide in an intelligent way the best course of action in the presence of an opposing force. The agents are deemed intelligent since they are able to optimize their actions in detriment of the opposing team.

The paper is organized as follows. Section 2 gives the background and required information from the single Defender problem [9]. In Section 2.1 we provide a root locus analysis of the polynomial equation that provides the optimal interception point. Section 3 further characterizes the solution of the individual ATDDG. The optimal strategies for the two-defender ATDDG with a dynamic Target are defined in Section 4. Illustrative examples are included in Section 5. The Game of Kind is solved in Section 6 and concluding remarks are made in Section 7.

2 Single Defender

This section presents the requisite properties of the Active Target Defense Differential Game (ATDDG), which was solved for a single Defender in Ref. [15]. The ATDDG comprises three agents, the Target (T), the Attacker (A), and the Defender (D) - see Fig. 1, whose (constant) speeds are given by V_T, V_A, and V_D.

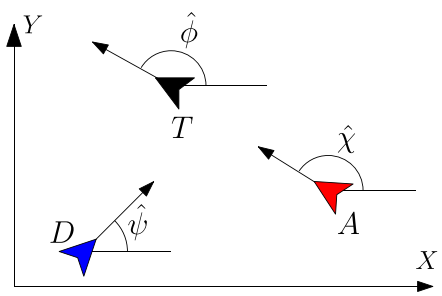

Fig. 1 Each agent's heading in the realistic frame for the single Defender ATDDG

The formulation herein assumes Beyond Visual Range scenarios where inter-agent altitude differences are negligible when compared to their separations in the latitude-longitude plane. Furthermore, we assume that the agents have "simple motion" in a plane given by the (normalized) kinematic equations

$$\dot{\hat{x}}_T = \alpha \cos\hat{\phi}, \qquad \hat{x}_T(0) = \hat{x}_{T_0} \tag{1}$$
$$\dot{\hat{y}}_T = \alpha \sin\hat{\phi}, \qquad \hat{y}_T(0) = \hat{y}_{T_0} \tag{2}$$
$$\dot{\hat{x}}_A = \cos\hat{\chi}, \qquad \hat{x}_A(0) = \hat{x}_{A_0} \tag{3}$$
$$\dot{\hat{y}}_A = \sin\hat{\chi}, \qquad \hat{y}_A(0) = \hat{y}_{A_0} \tag{4}$$
$$\dot{\hat{x}}_D = \cos\hat{\psi}, \qquad \hat{x}_D(0) = \hat{x}_{D_0} \tag{5}$$
$$\dot{\hat{y}}_D = \sin\hat{\psi}, \qquad \hat{y}_D(0) = \hat{y}_{D_0} \tag{6}$$

where $\alpha = V_T/V_A$ represents the speed ratio between T and A. For simplicity, we assume that D's speed is equal to A's speed.

The ATDDG involves full information, i.e., the system state, consisting of each agent's position $\hat{\mathbf{x}} := (\hat{x}_T, \hat{y}_T, \hat{x}_A, \hat{y}_A, \hat{x}_D, \hat{y}_D)$, is known by all agents. The agent's instantaneous headings $\hat{\phi}$, $\hat{\chi}$, and $\hat{\psi}$ comprise the control. Using the state $\hat{\mathbf{x}}$ each agent solves the differential game for the optimal headings for all agents.

Without loss of generality, we analyze the problem using the reduced state reference frame depicted in Fig. 2, where the $\hat{}$ is removed from the coordinates to differentiate from those expressed in the realistic frame. The reduced state reference frame is defined such that the X-axis passes through D and A, with $x_A > 0$ and $x_D = -x_A < 0$, and the Y-axis is aligned along the bisector between D and A. The points T and T' represent the initial and terminal positions of the Target, respectively. The reduced state, $\mathbf{x} = (x_A, x_T, y_T)$, can be obtained given any state $\hat{\mathbf{x}}$ in the realistic frame using the following coordinate transformation:

$$\begin{aligned}
x_A &:= \frac{1}{2}\sqrt{(\hat{x}_A - \hat{x}_D)^2 + (\hat{y}_A - \hat{y}_D)^2} \\
x_T &:= \frac{\left(\hat{x}_T - \frac{1}{2}(\hat{x}_A + \hat{x}_D)\right)(\hat{x}_A - \hat{x}_D) + \left(\hat{y}_T - \frac{1}{2}(\hat{y}_A + \hat{y}_D)\right)(\hat{y}_A - \hat{y}_D)}{\sqrt{(\hat{x}_A - \hat{x}_D)^2 + (\hat{y}_A - \hat{y}_D)^2}} \\
y_T &:= \frac{\left(\hat{y}_T - \frac{1}{2}(\hat{y}_A + \hat{y}_D)\right)(\hat{x}_A - \hat{x}_D) - \left(\hat{x}_T - \frac{1}{2}(\hat{x}_A + \hat{x}_D)\right)(\hat{y}_A - \hat{y}_D)}{\sqrt{(\hat{x}_A - \hat{x}_D)^2 + (\hat{y}_A - \hat{y}_D)^2}}.
\end{aligned} \tag{7}$$

The objective of the ATDDG is based on the terminal separation of the Target and Attacker, namely

$$d(t_f) = \sqrt{(x_A(t_f) - x_T(t_f))^2 + (y_A(t_f) - y_T(t_f))^2}, \tag{8}$$

which is the distance between the point T' and the Defender–Attacker intercept point I. The terminal time t_f is defined as the time instant where Defender intercepts the Attacker, and we restrict interception to point capture.[1] The solutions given in this paper consider only the initial conditions where capture of A by D is feasible, i.e., D intercepts A before A reaches the Target. The initial conditions that result in feasible solutions to the ATDDG are specified by the solution of the Game of Kind, see Refs. [10] and Section 6 within this paper.

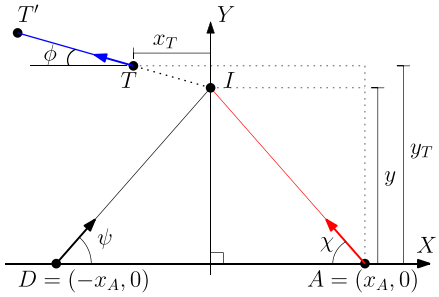

Fig. 2 Reduced state reference frame for the ATDDG when $x_T < 0$

[1] The assumptions that $V_D/V_A = 1$ and point capture cause the reachability boundaries for A with respect to D to be linear. The authors have investigated the single Defender cases when both these conditions are relaxed, and the results in this paper would extend using these cases [7, 8].

It has been shown in [15] that the ATDDG can be reformulated into an optimization problem over a single variable, which physically represents the aim-point for each agent. This optimal aimpoint is the A–D intercept point I in Fig. 2. The following Lemma explains how the aimpoint is found.

Lemma 1 *The optimal solution to the (single) active target defense differential game is as follows:*

- *When $x_T < 0$, A chooses its optimal aim-point, y^*, on the the bisector by minimizing the cost function (9). D's optimal aim-point is the same y^* as A. T's optimal control is to head directly away from y^*.*

$$J_l(y) = \alpha\sqrt{x_A^2 + y^2} + \sqrt{(y_T - y)^2 + x_T^2}. \quad (9)$$

- *When $x_T > 0$ and assuming a feasible solution exists,[2] T chooses its optimal aim-point, y^*, on the bisector by maximizing the cost function (10). A's optimal aim-point is the same y^* as T. D's optimal is aim at y^*.*

$$J_r(y) = \alpha\sqrt{x_A^2 + y^2} - \sqrt{(y_T - y)^2 + x_T^2}\ . \quad (10)$$

- *When $x_T = 0$, A and D's optimal aim-points are T's initial location y_T, and T's optimal heading is given by* Eq. 11.

$$\begin{aligned} \sin\phi &= \alpha\frac{y_T}{\sqrt{x_A^2+y_T^2}} \\ \cos\phi &= \frac{\sqrt{x_A^2+(1-\alpha^2)y_T^2}}{\sqrt{x_A^2+y_T^2}} \end{aligned} \quad (11)$$

In each case, if any agent deviates from this policy, then it is to their detriment. For proof, see Refs. [15].

Equations 9 and 10 are equal to the terminal distance (8). To see that $d(t_f) = J_l(y)$, note that the first term in Eq. 9 is equal to the distance between T' and T, and the latter term is the distance between T and I. In a like manner, $d(t_f) = J_r(y)$ when $x_T > 0$.

The minimum of Eq. 9 (maximum of Eq. 10) is found by differentiating with respect to y and setting the result equal to zero

$$\frac{dJ_l(y)}{dy} = \frac{\alpha y}{\sqrt{x_A^2 + y^2}} - \frac{y_T - y}{\sqrt{(y_T - y)^2 + x_T^2}} = 0 \quad (12)$$

$$\Rightarrow \frac{\alpha^2 y^2}{x_A^2 + y^2} = \frac{(y_T - y)^2}{(y_T - y)^2 + x_T^2} \quad (13)$$

$$(14)$$

which results in the quartic equation for $y \geq 0$

$$\begin{aligned} &(1-\alpha^2)y^4 - 2(1-\alpha^2)y_T y^3 \\ &+\left((1-\alpha^2)y_T^2 + x_A^2 - \alpha^2 x_T^2\right)y^2 - 2x_A^2 y_T y + x_A^2 y_T^2 = 0. \end{aligned} \quad (15)$$

The same quartic equation is obtained when the function (10) is differentiated in y and setting the resulting expression equal to zero. Another way to arrive at the quartic Eq. 15 is by synthesizing the saddle point optimal solution using the two-person extension of Pontryagin's Minimum Principle [2].

2.1 Root Locus

The following analysis shows existence of real solutions in Eq. 15, or equivalently (9) and (10). The domain of interest involves the parameter $0 \leq \alpha < 1$, which corresponds to the range of velocities for the target: $\alpha = 0$ for a static Target and $\alpha = 1$ when the Attacker's speed equals the Target's. Note when $\alpha = 1$, there is no game; the target eludes capture by traveling away from the Attacker.

Proposition 1 *For $0 \leq \alpha < 1$,* Eq. 15 *has only two real roots (corresponding to the minimizer of* Eq. 9 *and the maximizer of* Eq. 10*); one of these roots is less than or equal to y_T, while the other is greater than or equal to y_T. There are also two complex roots which are irrelevant to the game under study.*

Proof The proof follows a root locus analysis. For $\alpha = 0$, the four roots of the quartic (15) are: $y = y_T$,

[2] A feasible solution means that T is able to cross the bisector before being intercepted by A; this allows D to intercept A on the bisector. The existence of a feasible solution is prescribed by the solution of the Game of Kind, see Section 6.

$y = y_T$, and $y = \pm i x_A$, for all $x_T \in \mathbb{R}$ and $x_A > 0$, which holds by design in the reduced state frame. Differentiate the quartic (15) with respect to α

$$\begin{aligned}&\left\{2(1-\alpha^2)y^3 - 3(1-\alpha^2)y_T y^2\right.\\&+\left.\left[(1-\alpha^2)y_T^2 + x_A^2 - \alpha^2 x_T^2\right]y - x_A^2 y_T\right\}\frac{dy}{d\alpha}\\&-\alpha\left[y^4 - 2y_T y^3 + \left(x_T^2 + y_T^2\right)y^2\right] = 0. \end{aligned} \tag{16}$$

Setting $\alpha = 0$ and $y = y_T$ yields the relationship $0 \cdot \frac{dy}{d\alpha} = 0$, and $\frac{dy}{d\alpha}\big|_{\alpha=0}$ is indeterminate. Therefore, differentiate (16) with respect to alpha α and set $\alpha = 0$

$$\begin{aligned}&\left[2y^3 - 3y_T y^2 + \left(y_T^2 + x_A^2\right)y - x_A^2 y_T\right]\frac{d^2y}{d\alpha^2}\\&+\left(6y^2 - 6y_T y + x_A^2 + y_T^2\right)\left(\frac{dy}{d\alpha}\right)^2\\&-\left[y^4 - 2y_T y^3 + \left(x_T^2 + y_T^2\right)y^2\right] = 0. \end{aligned} \tag{17}$$

Set $\alpha = 0$ and $y = y_T$ in Eq. 16

$$0 \cdot \frac{d^2y}{d\alpha^2} + (x_A^2 + y_T^2)\left(\frac{dy}{d\alpha}\right)^2 = x_T^2 y_T^2 \tag{18}$$

$$\Rightarrow \quad \left.\frac{dy}{d\alpha}\right|_{\alpha=0, y=y_T} = \pm\frac{x_T y_T}{\sqrt{x_A^2 + y_T^2}}. \tag{19}$$

In the other extremity, $\alpha = 1$, Eq. 15 reduces to a quadratic equation whose roots are $y = \frac{x_A y_T}{x_A + x_T}$ and $y = \frac{x_A y_T}{x_A - x_T}$. If $x_T = \pm x_A$, then one of these roots is $y = +\infty$. This root becomes finite as α decreases, that is, $y < \infty$ for $\alpha = 1 - \epsilon$ for some small $\epsilon > 0$.

Setting $y = \pm i x_A$ in Eq. 16 yields

$$\left.\frac{dy}{d\alpha}\right|_{\alpha=0, y=\pm i x_A} = 0,$$

while substituting $y = \pm i x_A$ in Eq. 17 returns

$$\left[2x_A^2 y_T + \left(y_T^2 - x_A^2\right)y\right]\frac{d^2y}{d\alpha^2} = \left(x_A^2 - x_T^2 - y_T^2 + 2y_T y\right)x_A^2.$$

To determine $\frac{d^2y}{d\alpha^2}$, set $y = i x_A$ and $\frac{d^2y}{d\alpha^2} = a + ib$ and solve for a and b.

$$\left[2x_A^2 y_T + i x_A\left(y_T^2 - x_A^2\right)\right](a + ib) = \left(x_A^2 - x_T^2 - y_T^2 + 2i x_A y_T\right)x_A^2 \tag{20}$$

$$\Rightarrow \begin{bmatrix} 2x_A y_T & x_A^2 - y_T^2 \\ -\left(x_A^2 - y_T^2\right) & 2x_A y_T \end{bmatrix}\begin{bmatrix} a \\ b \end{bmatrix} = x_A\begin{bmatrix} x_A^2 - x_T^2 - y_T^2 \\ 2x_A y_T \end{bmatrix} \tag{21}$$

$$\Rightarrow \begin{bmatrix} a \\ b \end{bmatrix} = \frac{1}{\left(x_A^2 + y_T^2\right)^2}\begin{bmatrix} 2x_A y_T & -\left(x_A^2 - y_T^2\right) \\ x_A^2 - y_T^2 & 2x_A y_T \end{bmatrix}\begin{bmatrix} x_A^2 - x_T^2 - y_T^2 \\ 2x_A y_T \end{bmatrix}x_A \tag{22}$$

$$\Rightarrow \quad \begin{cases} a = -2\left(\frac{x_A x_T}{x_A^2 + y_T^2}\right)^2 y_T < 0 \\ b = \frac{\left(x_A^2 + y_T^2\right)^2 - \left(x_A^2 - y_T^2\right)x_T^2}{\left(x_A^2 + y_T^2\right)^2}x_A \end{cases} \tag{23}$$

Similarly, when $y = -i x_A$

$$\left[2x_A^2 y_T - i x_A\left(y_T^2 - x_A^2\right)\right](a + ib) = \left(x_A^2 - x_T^2 - y_T^2 - 2i x_A y_T\right)x_A^2 \tag{24}$$

$$\Rightarrow \begin{bmatrix} 2x_A y_T & -\left(x_A^2 - y_T^2\right) \\ x_A^2 - y_T^2 & 2x_A y_T \end{bmatrix}\begin{bmatrix} a \\ b \end{bmatrix} = x_A\begin{bmatrix} x_A^2 - x_T^2 - y_T^2 \\ -2x_A y_T \end{bmatrix} \tag{25}$$

$$\Rightarrow \quad \begin{cases} a = -2\left(\frac{x_A x_T}{x_A^2 + y_T^2}\right)^2 y_T < 0 & \text{as before!} \\ b = -\frac{\left(x_A^2 + y_T^2\right)^2 - \left(x_A^2 - y_T^2\right)x_T^2}{\left(x_A^2 + y_T^2\right)^2}x_A & \text{note sign inversion!} \end{cases}$$

So the two imaginary roots wander away from the real axis into the left hand side of the complex plane, whereas the two real roots split off at $y = y_T$ and move in opposite directions toward $\frac{x_A y_T}{x_A \pm x_T}$ along the real axis. The root-locus picture of the roots of the quartic Eq. 15 as a function of the problem parameter $0 \leq \alpha < 1$ is as shown in Fig. 3. Importantly, the quartic Eq. 15 has two complex roots and two real roots $y_1 \geq y_T$ and $y_2 \leq y_T$. □

3 Monotonicity of Eqs. 9 and 10

In order to determine the optimal solution for the case of a dynamic target, we first prove the monotonicity of the cost functions (9) and (10). These results are novel to this paper and are needed to determine the optimal strategies in Section 4.

Proposition 2 *Consider the case $x_T < 0$. The cost function (9) has only one minimum, which satisfies $0 < y^* < y_T$. Furthermore, the same function is monotone decreasing for $0 < y < y^*$, and it is monotone increasing for $y > y^*$.*

Proof The derivative of Eq. 9 is

$$J_l'(y) = \frac{\alpha y}{\sqrt{x_A^2 + y^2}} + \frac{y - y_T}{\sqrt{(y_T - y)^2 + x_T^2}}. \tag{26}$$

From Fig. 2 the headings of the Attacker and the Target are given by $\chi = \arctan \frac{y}{x_A}$ and $\phi = \arctan \frac{y_T - y}{-x_T} = \arctan \frac{y - y_T}{x_T}$, respectively. In addition, the distance from point A to point I is

$$\overline{AI} = \frac{y}{\sin \chi} \tag{27}$$

and the distance from point T to point I is given by

$$\overline{TI} = \frac{y_T - y}{\sin \phi} \tag{28}$$

Then, Eq. 26 can be written as follows

$$J_l'(y) = \frac{\alpha y}{\overline{AI}} + \frac{y - y_T}{\overline{TI}} = \alpha \sin \chi - \sin \phi. \tag{29}$$

Let us analyze the value of the cost function when $y = 0$. In this case, we have that $\chi = 0$ and $\phi = \arctan \frac{-y_T}{x_T}$, where $y_T > 0$ and $x_T < 0$. The Target's heading satisfies $0 < \phi < \frac{\pi}{2}$. Hence, the derivative of the cost satisfies $J_l'(0) = -\sin \phi < 0$. Now, at $y = y_T$ we have that $0 < \chi < \frac{\pi}{2}$, $\phi = 0$, and the derivative of Eq. 9 satisfies $J_l'(y_T) > 0$.

Because $J_l'(0) < 0$ and $J_l'(y_T) > 0$ the cost $J_l(y)$ has at least one minimum y^* that satisfies $0 < y^* < y_T$. Let $\chi^* = \arctan \frac{y^*}{x_A}$ and $\phi^* = \arctan \frac{y^* - y_T}{x_T}$. Then, $J_l'(y^*) = \alpha \sin \chi^* - \sin \phi^* = 0$.

We will now show monotonicity of the cost $J_l(y)$. Recall that the trigonometric function $\sin(\xi)$ is monotone increasing in the interval $\xi \in [-\pi/2, \pi/2]$. Also, the inverse trigonometric function $\arctan(m)$ is monotone increasing in the interval $m \in (-\infty, \infty)$.

For any y such that $0 < y < y^*$ we have that $0 < \chi(y) < \chi^*$ and $\phi^* < \phi(y) < \frac{\pi}{2}$. Then, the derivative of Eq. 9 satisfies $J_l'(y) = \alpha \sin \chi(y) - \sin \phi(y) < 0$ for $0 < y < y^*$.

Now, for any y such that $y^* < y < y_T$ we have that $0 < \chi^* < \chi(y) < \frac{\pi}{2}$ and $0 < \phi(y) < \phi^*$. Therefore, $J_l'(y) = \alpha \sin \chi(y) - \sin \phi(y) > 0$ for $y^* < y < y_T$.

Finally, since we use Euclidean distances $\overline{AI}$ and $\overline{TI}$, when $y > y_T$ the Target's heading is given by $\phi = \arctan \frac{y - y_T}{-x_T} = \arctan \frac{y_T - y}{x_T}$, and the distance between point T and point I is given by $\overline{TI} = \frac{y - y_T}{\sin \phi}$. Then, Eq. 26 can be written as follows

$$J_l'(y) = \frac{\alpha y}{\overline{AI}} + \frac{y - y_T}{\overline{TI}} = \alpha \sin \chi + \sin \phi. \tag{30}$$

Additionally, for any $y > y_T$ the Attacker's heading satisfies $0 < \chi^* < \chi(y) \leq \frac{\pi}{2}$ and the Target's heading satisfies $0 < \phi(y) \leq \frac{\pi}{2}$. Hence, $J_l'(y) = \alpha \sin \chi(y) + \sin \phi(y) > 0$ for $y > y_T$.

In conclusion, $J_l'(y) < 0$ for $0 < y < y^*$ and $J_l'(y) > 0$ for $y > y^*$ (since $J_l'(y_T) > 0$ as it was obtained at the beginning of this proof). Then the cost

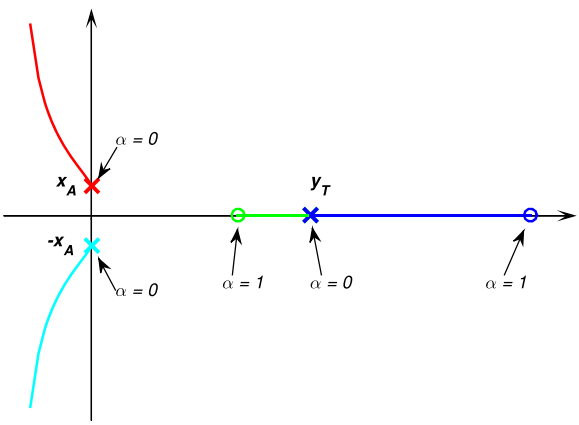

Fig. 3 Root Locus of the quartic (15) for $0 \leq \alpha < 1$

function (9) is monotone decreasing for $0 < y < y^*$ and it is monotone increasing for $y > y^*$, and the minimizer y^* satisfies $0 < y^* < y_T$. □

Proposition 3 *Consider the case* $0 < x_T < x_A$ *and let* $0 < \alpha < 1$. *The payoff function* (10) *has only one maximum, which satisfies* $y_T < y^* < \infty$. *Furthermore, the same function is monotone increasing for* $0 < y < y^*$, *and it is monotone decreasing for* $y > y^*$.

Proof Let us first obtain the first derivative of Eq. 10:

$$J_r'(y) = \frac{\alpha y}{\sqrt{x_A^2 + y^2}} - \frac{y - y_T}{\sqrt{(y - y_T)^2 + x_T^2}} \tag{31}$$

From Fig. 4 the headings of the Attacker and the Target are given by $\chi = \arctan \frac{y}{x_A}$ and $\phi = \arctan \frac{y - y_T}{x_T}$, respectively. In addition, the distance from point A to point I is

$$\overline{AI} = \frac{y}{\sin \chi} \tag{32}$$

and the distance from point T to point I is given by

$$\overline{TI} = \frac{y - y_T}{\sin \phi}. \tag{33}$$

Then, Eq. 31 can be written as follows

$$J_r'(y) = \frac{\alpha y}{\overline{AI}} - \frac{y - y_T}{\overline{TI}} = \alpha \sin \chi - \sin \phi. \tag{34}$$

First, let us analyze the payoff function at $y = y_T$ and the limit at $y \to \infty$. When $y = y_T$, we have that $\phi = 0$ and $\chi = \arctan \frac{y_T}{x_A}$, where $y_T > 0$ and $x_A > 0$. The Attacker's heading satisfies $0 < \chi(y_T) < \frac{\pi}{2}$. Hence, the derivative of Eq. 10 satisfies $J_r'(y_T) = \alpha \sin \chi > 0$. Now, as $y \to \infty$ we have that $\chi \to \frac{\pi}{2}$, $\phi \to \frac{\pi}{2}$, and the derivative of Eq. 10 satisfies $J_r'(\infty) = \alpha - 1 < 0$. Because $J_r'(y_T) > 0$ and $J_r'(\infty) < 0$ the payoff $J(y)$ has at least one maximum at y^* that satisfies $y_T < y^* < \infty$. Let $\chi^* = \arctan \frac{y^*}{x_A}$ and $\phi^* = \arctan \frac{y^* - y_T}{x_T}$. Then, $J_r'(y^*) = \alpha \sin \chi^* - \sin \phi^* = 0$.

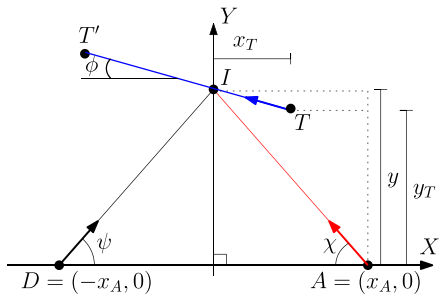

Fig. 4 Individual ATDDG for $x_T > 0$. The optimal aimpoint in this case is $y^* > y_T$

We will now show monotonicity of the payoff $J_r(y)$ defined in Eq. 10. Let us find the range of y such that $\phi(y) = \chi(y)$, where $0 < \phi, \chi < \infty$. Taking the tangent of ϕ and χ we have

$$\tan \phi(y) = \tan \chi(y) \Rightarrow \frac{y - y_T}{x_T} = \frac{y}{x_A}. \tag{35}$$

Define y_e as the value y that satisfies (35), namely:

$$y_e \triangleq \frac{x_A y_T}{x_A - x_T}. \tag{36}$$

Note that $y_e > y_T$ since $0 < x_T < x_A$. Also note that y_e is unique, that is, there is only one finite value of y such that $\phi(y) = \chi(y)$.

For $\epsilon > 0$, we have by Eq. 35

$$\begin{aligned} \frac{\epsilon}{x_T} > \frac{\epsilon}{x_A} &\Rightarrow \frac{\epsilon}{x_T} + \frac{y_e - y_T}{x_T} > \frac{\epsilon}{x_A} + \frac{y_e}{x_A} \\ &\Rightarrow \frac{y_e + \epsilon - y_T}{x_T} > \frac{y_e + \epsilon}{x_A} \end{aligned} \tag{37}$$

Let $y = y_e + \epsilon$, then the above inequality becomes

$$\frac{y - y_T}{x_T} > \frac{y}{x_A} \Rightarrow \frac{\pi}{2} > \phi(y) > \chi(y) > 0 \tag{38}$$

for any y, such that $y_e < y < \infty$ (because $y_e > y_T$ and $\epsilon > 0$). Similarly, for $y_T \le y < y_e$ we can show that $0 \le \phi(y) < \chi(y) < \frac{\pi}{2}$.

Additionally, note that $J_r'(y^*) = \alpha \sin \chi^* - \sin \phi^* = 0$ and $0 < \alpha < 1$, then $0 < \phi(y^*) < \chi(y^*) < \frac{\pi}{2}$. Altogether, $0 < y_T < y^* < y_e < \infty$.

1) Case $y \ge y_e$. We have that $J_r'(y) = \alpha \sin \chi(y) - \sin \phi(y) < 0$ since $\phi(y) \ge \chi(y)$ and $0 < \alpha < 1$. Hence, the payoff (10) is monotone decreasing in the interval $y \ge y_e$.
2) Case $y^* < y < y_e$. Let us compute the second derivative of Eq. 10

$$J_r''(y) = \alpha \cos \chi \frac{d\chi}{dy} - \cos \phi \frac{d\phi}{dy} \tag{39}$$

where

$$\frac{d\chi}{dy} = \frac{x_A}{x_A^2 + y^2} = \frac{\cos^2 \chi}{x_A} \tag{40}$$

$$\frac{d\phi}{dy} = \frac{x_T}{(y - y_T)^2 + x_T^2} = \frac{\cos^2 \phi}{x_T} \tag{41}$$

Then, we can write (39) as follows

$$J_r''(y) = \alpha \frac{\cos^3 \chi}{x_A} - \frac{\cos^3 \phi}{x_T} \tag{42}$$

Because $\phi(y) < \chi(y)$ for $y^* < y < y_e$, then $\cos\phi(y) > \cos\chi(y)$ and

$$\frac{\cos^3 \phi(y)}{x_T} > \alpha \frac{\cos^3 \chi(y)}{x_A} \tag{43}$$

Hence, $J_r''(y) < 0$ and the payoff is monotone decreasing for $y^* < y < y_e$.

3) Case $y_T \le y \le y^*$. For y in this range, $0 \le \phi(y) < \chi(y) < \frac{\pi}{2}$ and $J_r'(y_T) > 0$, as previously shown. Also, since $\phi(y) < \chi(y)$, we have that $J_r''(y) < 0$. Hence, the payoff is monotone increasing for $y_T \le y \le y^*$. Note that $J_r''(y^*) < 0$, as expected.
4) Case $0 < y < y_T$. Finally, since we use Euclidean distances $\overline{AI}$ and $\overline{TI}$, when $0 < y < y_T$ the Target's heading is given by $\phi = \arctan \frac{y_T - y}{x_T}$ and the distance between point T and point I is given by $\overline{TI} = \frac{y_T - y}{\sin\phi}$. Then, Eq. 31 can be written as follows

$$J_r'(y) = \frac{\alpha y}{\overline{AI}} - \frac{y - y_T}{\overline{TI}} = \alpha \sin\chi + \sin\phi \tag{44}$$

Additionally, for any $0 < y < y_T$ the Attacker's heading satisfies $0 < \chi(y) < \frac{\pi}{2}$ and the Target's heading satisfies $0 < \phi(y) < \frac{\pi}{2}$. Hence, $J_r'(y) = \alpha \sin\chi(y) + \sin\phi(y) > 0$ and the payoff is monotone increasing for $0 < y < y_T$.

In conclusion, the payoff (10) is monotone increasing for $0 < y < y^*$ and it is monotone decreasing for $y > y^*$, and the maximizer y^* satisfies $y_T < y^* < \infty$. □

4 Two Defender ATDDG

Consider the reduced state (x_A, x_T, y_T) reference frame in Fig. 2; in the two Defender ATDDG we will use two reduced state reference frames – one for each Defender. This geometry is depicted in Fig. 5. Note that the angle formed by the points D_1, A, and D_2 always satisfies $\angle D_1 A D_2 < \pi$, that is, the angle $\angle D_1 A D_2$ is the smaller angle, not the reflex angle.

The first reference frame is a function of A, T, and D_1; the corresponding reduced state is labeled as $(x_{A_1}, x_{T_1}, y_{T_1})$. The second reference frame is a function of A, T, and D_2; the corresponding reduced state is then labeled as $(x_{A_2}, x_{T_2}, y_{T_2})$.

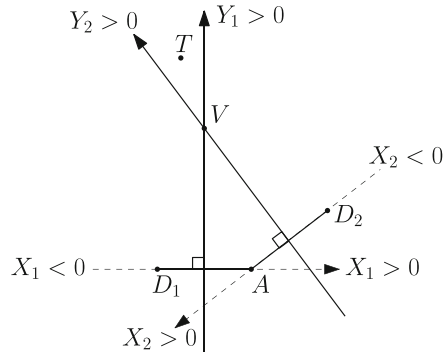

Fig. 5 Geometry for the ATDDG with two Defenders where two coordinate frames are drawn, one for each Defender

The reduced state coordinates for the single Defender ATDDG are defined such that the X-axis goes from D to A, namely $x_A > 0$ (thus $x_D = -x_A < 0$) and $y_T \ge 0$. This convention is maintained with two Defenders, i.e., the reference frame for each Defender is defined such that $x_{A_i} > 0$. In Fig. 5, the position of the target in the D_1 and D_2 frames is (x_{T_1}, y_{T_1}) and (x_{T_2}, y_{T_2}), respectively, and under this convention we have that $y_{T_1} > 0$, $x_{T_1} < 0$, $y_{T_2} > 0$, and $x_{T_2} < 0$. The bisectors for each reference frame intersect at the vertex point V.

We now investigate the optimal strategies of the two-Defender ATDDG when T is dynamic, i.e., $\alpha > 0$. The optimal strategies are obtained based on the single Defender ATDDG solutions, also called individual optimal solutions. Each individual solution y_1^*, y_2^* is obtained by rooting of the quartic (15) and using the corresponding state $(x_{A_1}, x_{T_1}, y_{T_1})$ or $(x_{A_2}, x_{T_2}, y_{T_2})$ The main goal in this section is to determine if, given the initial positions of T, A, D_1, D_2, either individual solution is still the optimal solution of the two defender ATDDG or if different strategies may further increase the terminal separation between T and A.

We will need the following definitions. The vertex V's coordinates in each of the reference frames, D_1 and D_2, are given by $(0, y_{V_1})$, $(0, y_{V_2})$, respectively (see Fig. 5). Let J_{l_1} (J_{r_1}) refer to the single Defender optimization problem $\min J_l(y)$ (or $\max J_r(y)$) in D_1's reference frame, when $x_{T_1} < 0$ ($x_{T_1} > 0$); similarly, J_{l_2} and J_{r_2} refer to these optimization problems in the D_2 frame. The optimal solution to J_{l_1} (J_{r_1}) or

J_{l_2} (J_{r_2}) will be given by y_1^* and y_2^*, where the specific optimization function J_{l_1} or J_{r_1} will be obvious from the context. Lastly, partition the space into the four regions shown in Fig. 6.

4.1 Optimal Solution When $T \in R_{V_c}$

In this case, $x_{T_1} < 0$ and $x_{T_2} < 0$, and the Attacker needs to solve a constrained minimization problem. The constraint is given by the vertex V imposed by the potential firing of two Defenders. The Attacker will find its new aim-point u^*. The Target's optimal policy is unchanged, that is, the Target's optimal heading is $v^* = u$.

Case A.1 ($y_{V_1} > y_1^*$ and $y_{V_2} > y_2^*$): The saddle point is $\arg\min\left\{J_{l_1}(y_1^*), J_{l_2}(y_2^*)\right\}$. By Proposition 2, any solution $y_1 \in (0, y_{V_1}]$ or $y_2 \in (0, y_{V_2}]$ that deviates from the optimal y_1^* and y_2^* is worse for A, i.e., $J_{l_1}(y_1) > J_{l_1}(y_1^*)$ and $J_{l_2}(y_2) > J_{l_2}(y_2^*)$. Thus, A's optimal aim-point is given by $u^* = \arg\min\left\{J_{l_1}(y_1^*), J_{l_2}(y_2^*)\right\}$, and due to Lemma 1, only the corresponding Defender is fired toward u^* and the Target cooperates with the fired Defender by running away from u^*.

Case A.2 ($y_{V_1} < y_1^*$ and $y_{V_2} < y_2^*$): The saddle point is V. The Attacker is constrained to choose an aim-point u such that $0 < u < y_{V_1}$ in reference frame D_1 and $0 < u < y_{V_2}$ in reference frame D_2. By Proposition 2, both cost functions, J_{l_1} and J_{l_2}, are monotone, thus the aim-point with minimum cost that satisfies the constraints is $u^* = y_{V_1} = y_{V_2}$, that is, the Attacker should aim at the vertex V. The Target runs away from V while both Defenders are fired aiming at V; both Defenders are needed to ensure A remains confined in R_A. It holds that $J_{l_1}(y_{V_1}) > J_{l_1}(y_1^*)$ and $J_{l_2}(y_{V_2}) > J_{l_2}(y_2^*)$, hence the Target benefits by firing two Defenders.

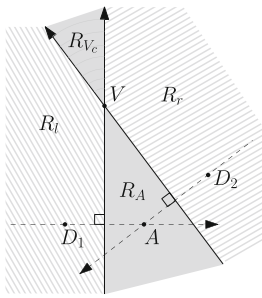

Fig. 6 Partition the space into the regions R_{V_c}, R_l, R_r, and R_A. The axes for the two reference frames, D_1 and D_2, are the same as in Fig. 5

Case A.3 ($y_{V_1} < y_1^*$ and $y_{V_2} > y_2^*$): The saddle point is y_2^*. We know from Proposition 2 that any point $y_2 \in (0, y_{V_2}] \setminus y_2^*$ causes $J_{l_2}(y_2) > J_{l_2}(y_2^*)$. We also know that $J_{l_1}(y_{V_1}) = J_{l_2}(y_{V_2})$. Thus by Proposition 2, $J_{l_1}(y_1) > J_{l_2}(y_2^*)$ for all $y_1 \in (0, y_{V_1}]$, that is, all y_1 in the feasible constraint region. Therefore, the Attacker's optimal aim-point is the individual solution $y_2^* = \arg\min_y J_{l_2}(y)$, and by Lemma 1, the Target runs away from y_2^*, while Defender 2 heads to this point to intercept A. Defender 1 is not fired since it will not reduce the cost attained by firing D_2 alone.

Case A.4 ($y_{V_1} > y_1^*$ and $y_{V_2} < y_2^*$): The saddle point is y_1^*. Its analysis follows that of Case A.3.

4.2 Optimal Solution When $T \in R_A$

In this case, $x_{T_1} > 0$ and $x_{T_2} > 0$, and the Target needs to solve a constrained maximization problem. The constraint is such that A is confined by the potential firing of two Defenders.

Case B.1 ($y_{V_1} > y_1^*$ and $y_{V_2} > y_2^*$): The optimal aim-point for the Target is $y^* = \arg\max_y\{J_{r_1}(y_1^*), J_{r_2}(y_2^*)\}$, which is also the optimal aim-point for A and the appropriate Defender. The proof follows Case A.2, when $T \in R_{V_c}$.

Case B.2 ($y_{V_1} < y_1^*$ and $y_{V_2} < y_2^*$): The saddle point is $y^* = \arg\max_y\{J_{r_1}(y_1^*), J_{r_2}(y_2^*)\}$. The proof follows Case *A.1*.

Case B.3 ($y_{V_1} < y_1^*$ and $y_{V_2} > y_2^*$): The saddle point is y_2^*. By Proposition 3, $J_{r_2}(y_2^*) > J_{r_2}(y_2)$ for all $y_2 \in (0, y_{V_2}]$ and $J_{r_1}(y_{V_1}) > J_{r_1}(y_1)$ for all $y_1 \in (0, y_{V_1}]$. We also know that $J_{r_1}(y_{V_1}) = J_{r_2}(y_{V_2})$. Thus, $y^* = y_2^*$ is the optimal aim-point for the Target, and by Lemma 1, A and D aim for this same location.

Case B.4 ($y_{V_1} > y_1^*$ and $y_{V_2} < y_2^*$): The saddle point is y_1^*. The proof follows Case B.3.

4.3 Optimal Solution When $T \in R_l$

In this case, $x_{T_1} < 0$ and $x_{T_2} > 0$. In the single agent problem with respect to Defender 2, D_2 maximizes J_{r_2}, while in the Defender 1 problem the Attacker would head to the minimum at $\arg\min J_{l_1}$. Again, we need to solve the constrained maximization problem

given these optimization criteria and the constraint on A's feasible region.

Case C.1 ($y_{V_1} > y_1^*$ and $y_{V_2} > y_2^*$): The saddle point is y_1^*. If the Attacker were to head toward an aim-point $y_2 \in (0, y_{V_2}]$, then in the two Defender scenario, the Target has a strategy to head away from this point due to the protective influence of Defender 1, which would be bad for A. In the single Defender scenario, this strategy was not an option, since the Target would remain on the Attacker's side. Thus the optimal strategy is given by Lemma 1, and the saddle point is y_1^* without firing Defender 2.

Case C.2 ($y_{V_1} < y_1^*$ and $y_{V_2} < y_2^*$): The saddle point is V. By Proposition 2 $J_{l_1}(y_{V_2}) < J_{l_1}(y_1)$ for any $y_1 \in (0, y_{V_1}]$, and by Proposition 3, $J_{r_2}(y_{V_2}) > J_{r_2}(y_2)$ for any $y_2 \in (0, y_{V_2}]$. Thus, the optimal saddle point, with respect to the constraint on the Attacker, is V, and both Defender 1 and 2 are fired.

Case C.3 ($y_{V_1} < y_1^*$ and $y_{V_2} > y_2^*$): This case will never occur, see Appendix.

Case C.4 ($y_{V_1} > y_1^*$ and $y_{V_2} < y_2^*$): The saddle point is y_1^*. If only D_1 is fired, then by Lemma 1 y_1^* is the optimal aim-point. If both D_1 and D_2 are fired, then y_1^* is still the optimal location, because D_2 cannot assist in constraining the Attacker. If only D_2 is fired, then the optimal trajectory for the Attacker crosses the protective boundary (bisector) created by D_1, since $y_{V_2} < y_2^*$. Thus T and D_1 cooperating is optimal, y_1^* is the saddle point, and D_2 is not fired.

4.4 Optimal Solution When $T \in R_r$

In this case $x_{T_1} < 0$ and $x_{T_2} > 0$, the solution is symmetric to the case of $T \in R_l$. The optimal strategies can be found by switching the policies of D_1 and D_2 in each case.

Remark 1 When the angle $\angle D_1AD_2$ satisfies $\frac{\pi}{2} \leq \angle D_1AD_2 < \pi$, Cases *A.1* and *B.2* will never occur. When this angle is acute, i.e., $0 < \angle D_1AD_2 < \frac{\pi}{2}$, Cases *C.1*-*C.2* will never occur. Lastly, as noted in Section 4.3, Case *C.3* will never occur. See Appendix for proof.

Remark 2 The degenerate cases when the two defenders and attacker are colinear, i.e., $\angle D_1AD_2 = 0$ or $\angle D_1AD_2 = \pi$, reduce to the single defender problem, where the optimal defender choice is that which results in the maximal final separation between the Attacker and Target.

5 Examples

Example 1: Static Target For a static target $\alpha = 0$, and the solution to the single Defender ATDDG is solely prescribed by the aim-point of the Defender and Attacker.

In Fig. 7 the region is divided into four partitions: R_1, R_A, R_2, and R_V. The Attacker is able to reach all points in partition R_A before either Defender. Partitions R_1, R_2, and R_V define the regions where Defender 1 or Defender 2 can reach before the Attacker.

Case 1 (and 2): The target is in partition R_1 (R_2). The closest point to the Target that the Attacker can reach before being intercepted by a Defender is the point on the bisector that is closest to the Target.

In this case, the closest point to the Target that the Attacker can reach before being intercepted by a Defender is the point on the bisector that is closest to the Target. Mathematically, this is the point, $I = (0, y_{T_1})$. In other words, the Attacker and Defender 1 (Defender 2) both head towards the projection of the Target onto the bisector. If the Target is in R_1 (R_2), the Attacker and D_1 (D_2) head towards the point y_{T_1} (y_{T_2}).

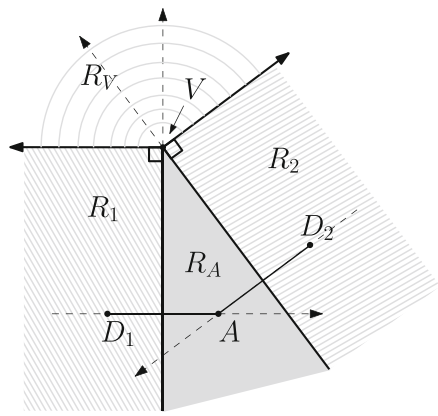

Fig. 7 Example 1: Partitioning the solution space for the static target two Defender game.

Case 3: The target is in partition R_V. This scenario shows the benefit of having two Defenders. Because there are two Defenders, the Attacker is confined to partition R_A. The closest point of to the Target that the Attacker can reach is V. In this scenario, both Defenders and the Attacker head towards V.

Case 4: The target is in partition R_A. All points in partition R_A can be reached by the Attacker before Defender 1 or Defender 2. Therefore, in this case the Attacker wins.

Example 2 The coordinates of the Target and the Attacker are $T = (-1, 14)$ and $A = (1, 2)$. Two Defenders can be potentially fired from the coordinates $D_1 = (-7, 4)$ and $D_2 = (8, 7)$. These initial positions are shown in Fig. 8a. The Attacker and the Defenders have unit speed. The Target's speed is $V_T = 0.6$. The speed ratio parameter $\alpha = 0.6$ and the initial positions of all agents in the fixed Cartesian frame are all the data necessary to solve the problem.

With this information we can solve the quartic Eq. 15 twice (once for each Defender) to obtain the individual optimal solutions with respect to each individual coordinate frame. These solutions are $y_1^* = 10.665$ and $y_2^* = 10.233$ and they correspond to points in the fixed frame given by $(-0.413, 13.347)$ and $(-1.447, 12.827)$ which are also shown in Fig. 8a. The location of the Vertex is given by the intersection of the orthogonal bisectors of $\overline{D_1 A}$ and $\overline{D_2 A}$ which is the point $V = (-0.778, 11.889)$. Figure 8a shows the position of the four agents, the two orthogonal bisectors, the individual solutions, and the location of the vertex. It can be seen that the Target is located in Region R_{V_c}.

From the Vertex coordinates we obtain that $y_{V_1} = 9.162$ and $y_{V_2} = 9.080$ and the applicable case is $A.2$ since $y_{V_1} < y_1^*$ and $y_{V_2} < y_2^*$. Therefore, the Attacker aims at the vertex where it is intercepted by both D_1 and D_2 and it attains its minimum cost subject to the constraints imposed by the presence of both Defenders. The optimal trajectories are shown in Fig. 8b.

Example 3 Unlike Example 2 where the initial positions were chosen as integer values, the initial positions for each agent in this example were chosen randomly (each with different distributions) and rounded to 3 decimal places. The coordinates of the Target and the Attacker are $T = (0.823, -0.507)$ and $A = (-4.328, -0.735)$. Two Defenders can be potentially fired from the coordinates $D_1 = (-1.435, -4.628)$ and $D_2 = (-2.176, 4.293)$. The speed ratio is $\alpha = 0.6$. From this initial data we calculate that the x-coordinate of the Target in each individual frame is $x_{T_1} = -0.464$ and $x_{T_2} = 0.498$. We can also calculate the individual optimal solutions $y_1^* = 3.993$ and $y_2^* = 4.953$ which correspond to the points in the fixed

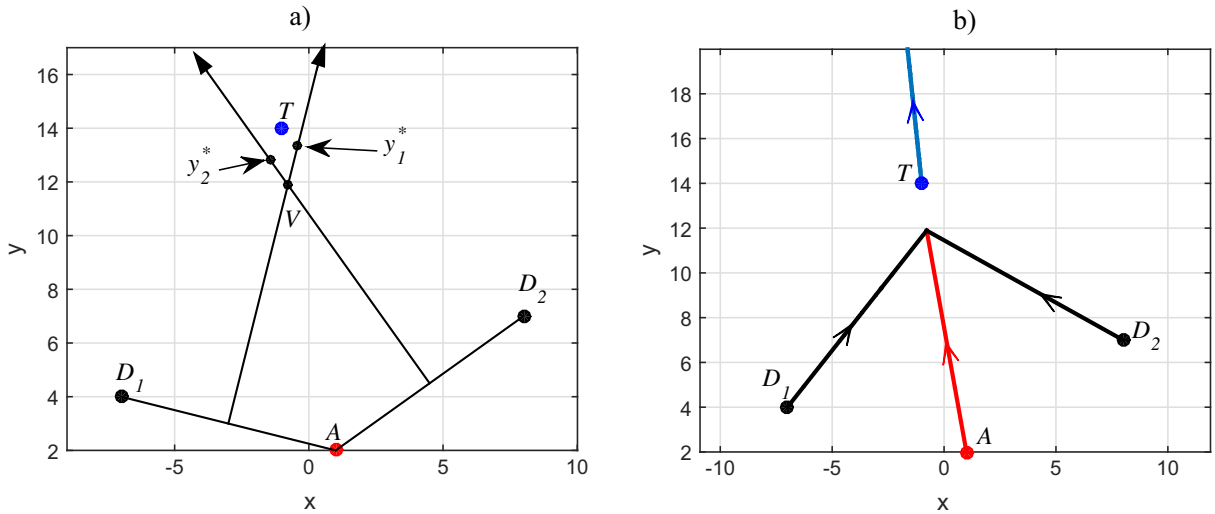

Fig. 8 Example 2: **a**) initial positions of the Target, the Attacker, and the two Defenders and locations of individual optimal aimpoints and vertex. **b**) Optimal trajectories where the Attacker is simultaneously intercepted by both Defenders

frame given by (0.323, −0.299) and (1.302, −0.170), respectively. The location of the Vertex is given by the intersection of the orthogonal bisectors of $\overline{D_1 A}$ and $\overline{D_2 A}$ which is the point $V = (0.792, 0.048)$. Fig. 9a shows the position of the four agents, the two orthogonal bisectors, the individual solutions, and the location of the vertex.

We obtain the Vertex coordinates in each individual frame $y_{V_1} = 4.576$ and $y_{V_2} = 4.399$ and the applicable case in this example is $C.4$ since $x_{T_1} < 0, x_{T_2} > 0$, $y_{V_1} > y_1^*$ and $y_{V_2} < y_2^*$. Therefore, the Attacker aims at the individual optimal solution y_1^* where it is intercepted by D_1 only, that is, D_2 is not capable or reducing the cost attained by the individual solution $y_1^*$and is not fired. The optimal trajectories are shown in Fig. 8b.

6 Game of Kind

In previous sections we were concerned with the Game of Degree of the ATDDG: The Target and Defender not only envision interception of the Attacker (and survival of the Target) but they also strive to maximize a payoff, the terminal separation between Target and Attacker. The Game of Degree is played for initial conditions where survival of the Target is guaranteed and it returns a real number, the Value of the game.

On the other hand, the Game of Kind provides a binary answer (yes or no) to the question: Can the Target be captured given some initial state? The notions of Game of Degree and Game of Kind are common in pursuit and evasion games [14]. The solution of the Game of Kind provides the subset of the state in which it is possible to actually play the Game of Degree.

In addition to providing the solution to the Game of Degree of the ATDDG, we also aim at solving the Game of Kind. This section discusses this aspect and its importance in the design of plans for defense of valuable targets.

The ATTDG described in Section 2 addresses a three agent engagement scenario. In such a problem, the Target will evade the Attacker with the help of the Defender which strives to intercept the Attacker. In combat and other military missions there exist phases or situations that occur previous to the three body engagement presented in this paper. An early phase, from the point of view of the T/D team, is related to the relative T/D configuration before the detection of the Attacker. Moreover, it is beneficial for the Target/Defender team to determine best strategies for motion planning prior to the encounter of an Attacker missile. The Defender, in this sense, is not specifically the Defender missile but the friendly UAV that is tasked to protect the Target aircraft by firing the Defender missile.

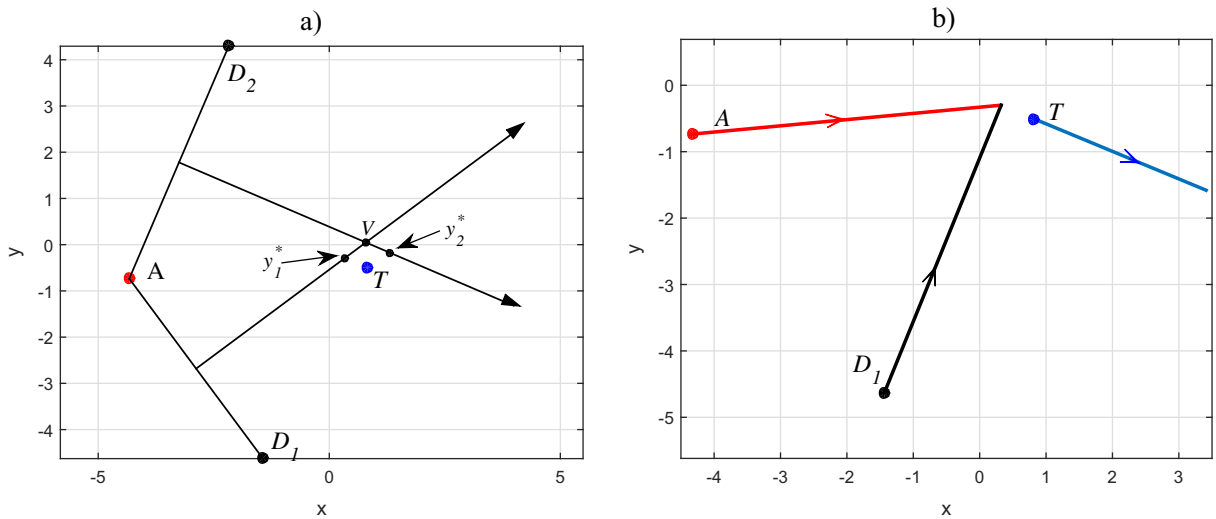

Fig. 9 Example 3: **a**) initial positions of the Target, the Attacker, and the two Defenders and locations of individual optimal aimpoints and vertex. **b**) Optimal trajectories where the Attacker is only intercepted by Defender 1

In this section we provide a characterization of the winning regions of the Attacker and of the Target/Defender team, that is, we determine if A will capture T or if A is intercepted by D before it can reach T given the initial positions of each agent; hence it is a solution to the Game of Kind. This study can also be seen as a formulation of the Target's vulnerability region based on the possible presence of an Attacker missile. The parameters are the separation between Target and Defender $d_{DT} > 0$ and the Target's speed ratio $0 < \alpha < 1$. The objective is to characterize the curve $F(x, y) = 0$ that delimits the winning region of the Attacker. The determination of the Attacker winning region or the Target's vulnerability region represents an important step towards the planning and implementation of cooperative Target/wingman trajectories under uncertainty of Attacker launching platforms.

Let us consider, without loss of generality, the coordinate frame shown in Fig. 10 where

$$x_D = -d_{DT}. \tag{45}$$

If a solution exists to the ATDDG, then, the Defender intercepts an hypothetical Attacker, located at generic coordinates (x, y), at the orthogonal bisector of the line $\overline{AD}$ which we denote as Y_o. The Target (when it is initially on the Attacker's side of the line Y_o) escapes the Attacker if it is able to cross Y_o and reach the Defender's side of Y_o. Given the initial separation between Target and Defender d_{DT}, the Attacker

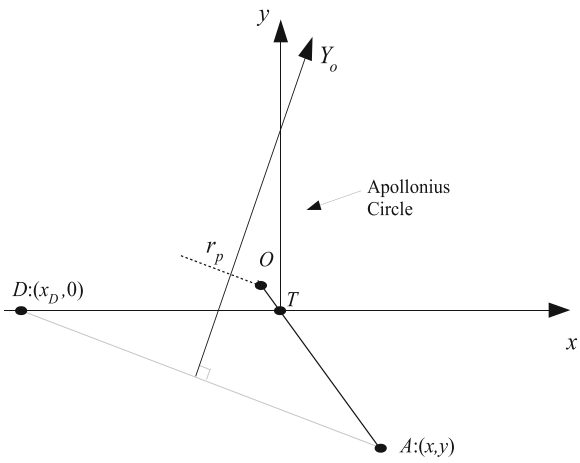

Fig. 10 Configuration of the ATDDG to solve the Game of Kind

coordinates (x, y), and the speed ratio α, the condition for the Target's survival is that the Apollonius circle between the Attacker and the Target intersects the orthogonal bisector Y_o.

A circle is alternatively defined as the set of points P that have a constant ratio of distances to two given points (also called foci) A and T, i.e., $\alpha = \frac{\overline{TP}}{\overline{AP}}$ is constant. The circle defined in this way is referred to as the Apollonius circle and it is an important tool to analyze pursuit problems. In detail, A and T travel in straight lines at constant speeds V_A and V_T, respectively, where the constant $\alpha = \frac{V_T}{V_A}$ and A strives to intercept T. A intercepts T at a point on the Apollonius circle and at that point the distance traveled by T is equal to α times the distance traveled by A. Hence, an Apollonius circle can be constructed based on the speed ratio α and on the distance between the Attacker and the Target. The radius of the circle is denoted by r_p and its center is denoted by O. The points A, T, and O are collinear.

Theorem 1 *The boundary of the Attacker winning region is given by the* (x, y) *Cartesian coordinates which satisfy the following*

$$y = \pm\sqrt{\frac{-c_1 - \sqrt{c_1^2 - 4c_0c_2}}{2c_0}} \tag{46}$$

where

$$\begin{aligned} c_0 &= 1 - \alpha^2 \\ c_1 &= 2\left((1-\alpha^2)x^2 + 2\alpha^2 x_D x + \frac{\alpha^4 - 2\alpha^2 - 1}{1-\alpha^2}x_D^2\right) \\ c_2 &= (1-\alpha^2)\left(x_D^4 + x^4\right) + 4\alpha^2 x_D x\left(x_D^2 + x^2\right) \\ &\quad -2(3\alpha^2+1)x_D^2x^2. \end{aligned} \tag{47}$$

Proof The critical point for survival is when the Apollonius circle is tangent to Y_o as it is shown in Fig. 11. In order to determine every initial position of the Attacker such that (given d_{DT} and α) this condition holds, we proceed as follows. Define the angle $\xi = \theta - \eta$, where θ is the Line-Of-Sight (LOS) angle from T to A and η is the LOS angle from D to A. Let the position of the Attacker be given by $A : (x, y)$ and define $r = \sqrt{x^2 + y^2}$. The radius of the Apollonius circle is given by $r_p = \frac{\alpha}{1-\alpha^2}r$. The distance from A to the center O of the Apollonius circle is $d_{AO} = \frac{1}{1-\alpha^2}r$.

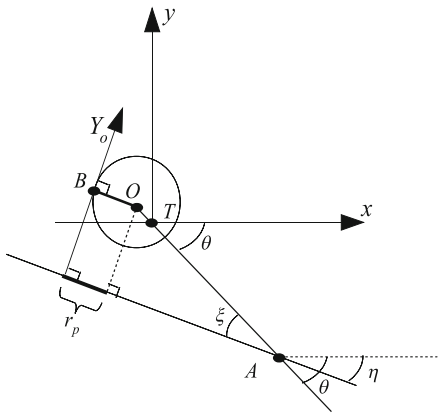

Fig. 11 The case where the Apollonius circle is tangent to the orthogonal bisector determines the barrier that separates the winning regions of each team

The condition that the Apollonius circle is tangent to Y_o can be written as

$$d_{OB} = r_p \tag{48}$$

where d_{OB} represents the distance from the center of the Apollonius circle to the tangent point which is denoted by B. We note that when the Apollonius circle is tangent to Y_o then the line $\overline{OB}$ is parallel to the line $\overline{AD}$; then, condition (48) can be recast as follows

$$\frac{1}{2}d_{AD} - d_{AO}\cos\xi = r_p \tag{49}$$

which can also be written as

$$\frac{1}{2}d_{AD} - \frac{1}{1-\alpha^2}r(\cos\theta\cos\eta + \sin\theta\sin\eta) = \frac{\alpha}{1-\alpha^2}r \tag{50}$$

where $d_{AD}^2 = r^2 + x_D^2 - 2x_D x$.

Let us note that $\cos\eta = \frac{x-x_D}{d_{AD}}$ and $\sin\eta = \frac{y}{d_{AD}}$. Then, Eq. 50 is now given by

$$\frac{1}{2}d_{AD} - \frac{1}{1-\alpha^2}\frac{1}{d_{AD}}(r^2 - x_D x) = \frac{\alpha}{1-\alpha^2}r. \tag{51}$$

Multiplying both sides of Eq. 51 by $2(1-\alpha^2)d_{AD}$ and simplifying terms we obtain

$$-(1+\alpha^2)r^2 + (1-\alpha^2)x_D^2 + 2\alpha^2 x_D x = 2\alpha r\sqrt{r^2 + x_D^2 - 2x_D x}. \tag{52}$$

Taking the square of both sides of Eq. 52 and combining the resulting terms we get the following equation

$$\begin{aligned}(1-\alpha^2)^2 r^4 &+ \left(4\alpha^2(1-\alpha^2)x_D x + 2(\alpha^4 - 2\alpha^2 - 1)x_D^2\right)r^2 \\ &+ 4\alpha^4 x_D^2 x^2 + 4\alpha^2(1-\alpha^2)x_D^3 x \\ &+ (1-\alpha^2)^2 x_D^4 = 0\end{aligned} \tag{53}$$

Finally, we substitute $r^2 = x^2 + y^2$ in Eq. 53 and after further simplification we obtain

$$\begin{aligned}&(1-\alpha^2)y^4 + 2\left((1-\alpha^2)x^2 + 2\alpha^2 x_D x + \frac{\alpha^4 - 2\alpha^2 - 1}{1-\alpha^2}x_D^2\right)y^2 \\ &+(1-\alpha^2)\left(x_D^4 + x^4\right) + 4\alpha^2 x_D x\left(x_D^2 + x^2\right) \\ &-2(3\alpha^2 + 1)x_D^2 x^2 = 0.\end{aligned} \tag{54}$$

Equation 54 is a fourth-order equation in both x and y. However the coordinate y only appears as y^4 and y^2, then, we can see Eq. 54 as a quadratic equation in y^2 where the solutions are given by

$$y_1^2 = \frac{-c_1 - \sqrt{c_1^2 - 4c_0 c_2}}{2c_0} \tag{55}$$

$$y_2^2 = \frac{-c_1 + \sqrt{c_1^2 - 4c_0 c_2}}{2c_0}. \tag{56}$$

Additionally, both solutions, y_1^2 and y_2^2, are continuous functions of x.

One can demonstrate which one of these solutions is applicable to our problem. In the particular case where $x = x_D$ the applicable solution is $y^2 = 0$. In such a case we can see that $y_1^2 = 0$ whereas $y_2^2 = (\frac{2\alpha}{1-\alpha^2}x_D)^2 \neq 0$. Hence, the applicable solution is Eq. 55.

Because of the symmetry of the configuration along the x-axis of the coordinate frame in Fig. 10 both solutions, $y_1 = \pm\sqrt{y_1^2}$, apply to our problem. □

Figure 12 shows several examples using different values for the parameters d_{DT} and α.

6.1 Attacker Winning Regions with Two Defenders

It can be seen from Theorem 1 that the vulnerability region of the Target can be reduced by decreasing the distance d_{DT}. In many mission scenarios the separation d_{DT} cannot be arbitrarily decreased because of

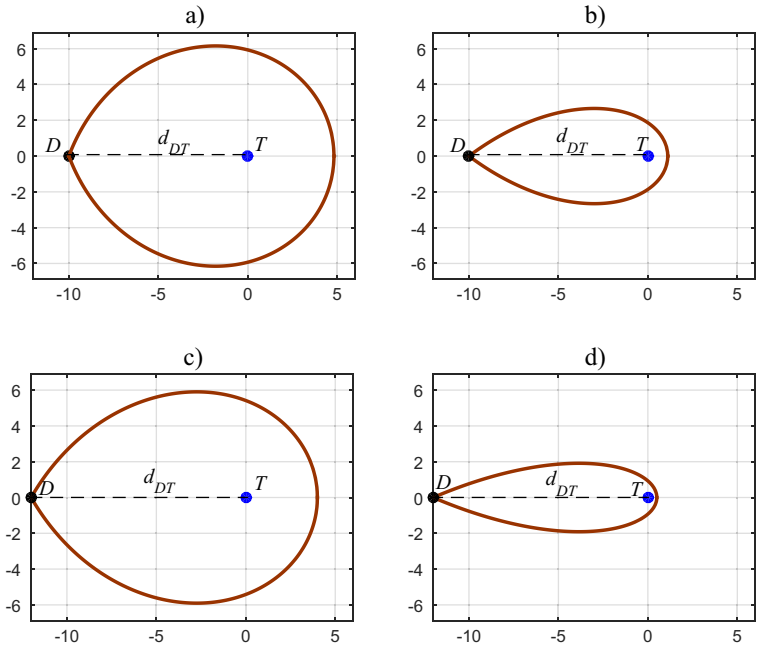

Fig. 12 Examples of vulnerability regions: **a**) $d_{DT} = 10, \alpha = 0.35$. **b**) $d_{DT} = 10, \alpha = 0.8$. **c**) $d_{DT} = 12, \alpha = 0.5$. **d**) $d_{DT} = 12, \alpha = 0.92$

different mission specifications such as maintaining a safe separation to avoid fraternal damage. It also may occur that the friendly UAV that is in charge of firing the Defender is also assigned to perform other tasks which makes the separation d_{DT} to increase allowing a larger Target vulnerability region.

The presence of two friendly UAVs that are capable of firing a Defender missile each represents a significant advantage in terms of protecting the Target not only during the TAD engagement but also to reduce the Target vulnerability area prior to the encounter of an Attacker missile. With respect to Fig. 13, the presence of D_1 generates the vulnerability region R_1. When only D_2 is present, the vulnerability region is R_2. However, when both D_1 and D_2 are capable of firing a Defender missile each the Target vulnerability region (or the Attacker winning region) is

$$R_A = R_1 \bigcap R_2. \tag{57}$$

This means that A can only win if it is initially located inside R_A. Otherwise, there exists an strategy for T to cooperate with D_1 or D_2 such that A will be intercepted and T escapes A's pursuit. Thus, the presence of a second friendly UAV which is able to assist the Target by firing D_2 is beneficial to the Target since its vulnerability region can be significantly reduced. This region is given by the intersection of the regions by each Defender whose boundaries are defined according to Eq. 46. This is so because D_2 can assist the Target and intercept an Attacker which is located at $A = (x, y)$ for $A \notin R_2$. This includes any point $\{A \in R_1 | A \notin R_A\}$. This means that the Target cooperates with D_2 when the Attacker is located outside the R_2 vulnerability region but inside the R_1 vulnerability region and vice versa. Therefore, the

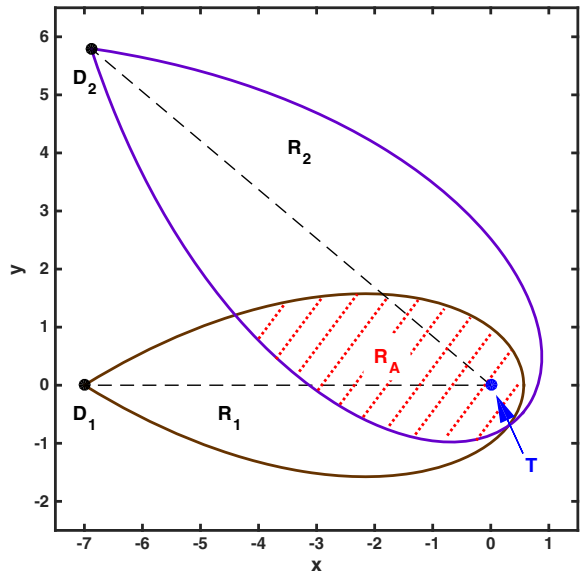

Fig. 13 Vulnerability regions with two Defenders: $\alpha = 0.85$, $d_{D_1T} = 7$, $d_{D_2T} = 9$ and $\angle D_1 T D_2 = 0.7$ rad

vulnerability region is reduced to the intersection of the individual regions.

7 Conclusions

This paper addressed the two-defender active target defense differential game (ATDDG). It was shown that under certain initial conditions the Target UAV sees its payoff increased (final Target-Attacker separation increases) by firing an auxiliary Defender missile. Based on the solutions of the individual ATDDG, the presence of two Defenders entails the formulation of a constrained optimization problem. As it is expected, the presence of two well-positioned Defenders results in faster interception of the Attacker compared to the case of only one Defender. The Attacker is left to determine its optimal heading subject to constraints imposed by the second Defender in order to minimize the final separation with respect to the Target. The Target and Defenders cooperate in order for the Defenders to intercept the Attacker while maximizing the terminal Target-Attacker distance. The Game of Kind that determines the Target's area of vulnerability was solved in this paper as well. Finally, it was shown that the presence of two friendly UAVs capable of assisting the Target by firing a Defender each represents a significant benefit since the Target's area of vulnerability can be greatly decreased.

Acknowledgements The authors would like to thank Prof. Tamer Basar for the fruitful conversations leading to this work.

Appendix

In this Appendix, proof is given why certain cases in Section 4 will never occur.

Proposition 4 *Case A.1: When $x_{T_1} < 0$ and $x_{T_2} < 0$ (i.e., $T \in R_{V_c}$) and $\frac{\pi}{2} \leq \angle D_1 A D_2 < \pi$, it is never the case that both $y_{V_1} > y_1^*$ and $y_{V_2} > y_2^*$.*

Proof Consider the range of optimal solutions to $\min J_l(y)$, which are depicted in Fig. 14. It only makes sense to consider speed ratios in the range $\alpha \in [0, 1)$, because when $\alpha \geq 1$, the Target is guaranteed to escape, and there is no active defense differential

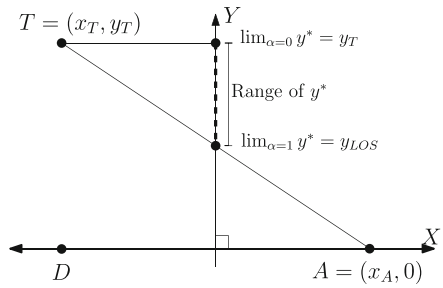

Fig. 14 Feasible range of y^* when $x_T < 0$

game. In the case of the static target ($\alpha = 0$), $y^* = y_T$, whereas the optimal aim-point y^* when $\alpha = 1$ is the attacker's line-of-sight intersection on the bisector

$$y^* = y_{LOS} = \frac{x_A y_T}{x_A - x_T}. \tag{58}$$

Thus, the optimal aim-point, when $x_T < 0$, must be in the range $y^* \in [y_{LOS}, y_T)$.

Consider the case where $T \in R_{V_c}$ is to the right of the line-of-sight vector from A to V, as shown in Fig. 15. For any initial Target location inside this region, the optimal solution $y_1^* = \min J_l(y)$ must be greater than V, with equality occurring when T falls on the line-of-sight vector and $\alpha = 1$, i.e., $y_{LOS} > V$ when $0 \leq \alpha < 1$. The reverse is true if T were to the left side of the line-of-sight vector, where y_2^* would then be greater than V. Thus is impossible for both $y_{V_1} > y_1^*$ and $y_{V_2} > y_2^*$; one of them must be greater than V when $T \in R_{V_c}$. □

Proposition 5 *Case B.2: When $x_{T_1} > 0$ and $x_{T_2} > 0$ (i.e., $T \in R_A$) and $\frac{\pi}{2} \leq \angle D_1 A D_2 < \pi$, it is never the case that both $y_{V_1} < y_1^*$ and $y_{V_2} < y_2^*$.*

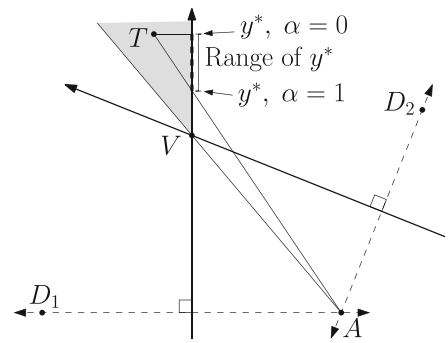

Fig. 15 If $x_{T_1} < 0$ and $x_{T_2} < 0$, then it is impossible for $y_{V_1} > y_1^*$ and $y_{V_2} > y_2^*$

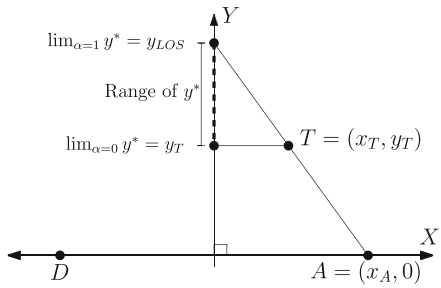

Fig. 16 Feasible range of y^* when $x_T > 0$

Proof A similar argument to that of Case A.1 can be made here using the geometry shown in Figs. 16 and 17. □

Proposition 6 *Case C.3: When $x_{T_1} < 0$ and $x_{T_2} > 0$ (i.e., $T \in R_l$) and $\frac{\pi}{2} \leq \angle D_1 A D_2 < \pi$, it is never the case that $y_{V_1} < y_1^*$ and $y_{V_2} > y_2^*$.*

Proof In order to guarantee for $0 \leq \alpha < 1$ that $y_1^* > y_{V_1}$, by the geometry in Fig. 14 it must be true that $T \in R_{V_1} \subset R_l$. Furthermore when $T \in R_{V_1}$, by the geometry in Fig. 16 y_2^* must be greater than V. Thus, the case $y_{V_1} < y_1^*$ and $y_{V_2} > y_2^*$ will never occur when $T \in R_l$. □

Proposition 7 *When $x_{T_1} < 0$ and $x_{T_2} > 0$ (i.e., $T \in R_l$), $0 < \angle D_1 A D_2 < \frac{\pi}{2}$ and the vertex V is inside the (acute) angle $\angle D_1 A D_2$, then cases C.1-C.3 will never occur.*

Proof By the geometry in Figs. 16 and 18, when $0 \leq \alpha < 1$ and since $x_{T_2} > 0$, then $y_{V_2} < y_2^*$. Thus cases *C.1* and *C.3* will never occur. Furthermore,

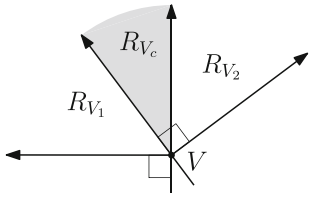

Fig. 17 A zoomed in view of Fig. 7. R_{V_c} is partitioned by the bisectors of A-D_1 and A-D_2; the outside boundaries of R_{V_1} and R_{V_2} are perpendicular to these bisectors

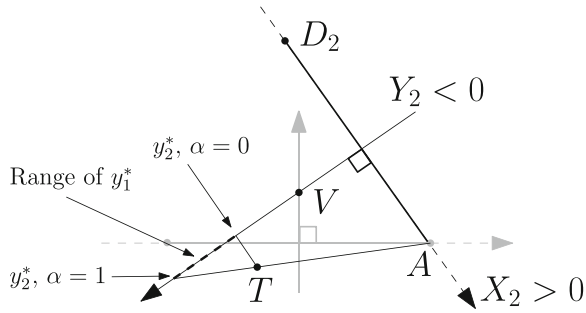

Fig. 18 Scenario where $\angle D_1 A D_2 < \frac{\pi}{2}$ and V is inside said angle. Note that y_2^* must satisfy $y_{V_2} < y_2^*$ for any $\alpha \in [0, 1)$

considering the Figs. 14 and 19, when $0 \leq \alpha < 1$ and since $x_{T_1} < 0$, then $y_{V_1} > y_1^*$. Thus case *C.2* will never occur. □

Proposition 8 *When $x_{T_1} < 0$ and $x_{T_2} > 0$ (i.e., $T \in R_l$), $0 < \angle D_1 A D_2 < \frac{\pi}{2}$ and the vertex V is outside the (acute) angle $\angle D_1 A D_2$ (see Fig. 20), then cases C.1-C.3 will never occur (Table 1).*

Proof The proof follows that of Proposition 7. □

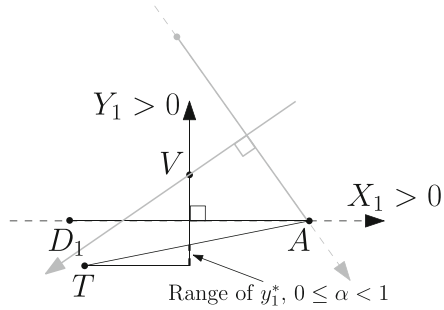

Fig. 19 $\angle D_1 A D_2 < \frac{\pi}{2}$ and V is inside said angle. Note that y_1^* must satisfy $y_{V_1} > y_1^*$ for any $\alpha \in [0, 1)$

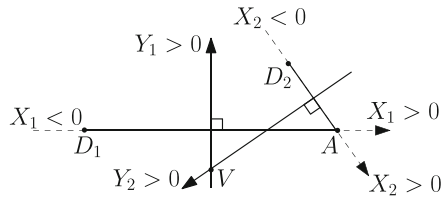

Fig. 20 V lies outside $\angle D_1 A D_2$ and $0 < \angle D_1 A D_2 < \frac{\pi}{2}$

Table 1 Summary of Two-Defender Optimal Strategies (DNO:Does Not Occur)

Case	$0 < \angle D_1AD_2 < \frac{\pi}{2}$	$\frac{\pi}{2} \leq \angle D_1AD_2 \leq \pi$
A.1	$\arg\min\left\{J_{l_1}(y_1^*), J_{l_2}(y_2^*)\right\}$	DNO
A.2	V	V
A.3	y_2^*	y_2^*
A.4	y_1^*	y_1^*
B.1	$\arg\max\left\{J_{r_1}(y_1^*), J_{r_2}(y_2^*)\right\}$	$\arg\max\left\{J_{r_1}(y_1^*), J_{r_2}(y_2^*)\right\}$
B.2	$\arg\max\left\{J_{r_1}(y_1^*), J_{r_2}(y_2^*)\right\}$	DNO
B.3	y_2^*	y_2^*
B.4	y_1^*	y_1^*
C.1	DNO	y_1^*
C.2	DNO	V
C.3	DNO	DNO
C.4	y_1^*	y_1^*

References

1. Bakolas, E., Tsiotras, P.: Optimal pursuit of moving targets using dynamic Voronoi diagrams. In: 49th IEEE Conference on Decision and Control, pp. 7431–7436 (2010)
2. Basar, T., Olsder, G.J.: Dynamic noncooperative game theory. In: Classics in Applied Mathemetics, vol. 23. Society for Industrial and Applied Mathematics (SIAM) (1999)
3. Casbeer, D.W., Garcia, E., Pachter, M.: The target differential game with two defenders. In: International Conference on Unmanned Aircraft Systems (2016)
4. Earl, M.G., D'Andrea, R.: A decomposition approach to multi-vehicle cooperative control. Robot. Auton. Syst. **55**(4), 276–291 (2007)
5. Fuchs, Z.E., Khargonekar, P.P., Evers, J.: Cooperative defense within a single-pursuer, two-evader pursuit evasion differential game. In: 49th IEEE Conference on Decision and Control, pp. 3091–3097 (2010)
6. Ganebny, S.A., Kumkov, S.S., Le Ménec, S., Patsko, V.S.: Model problem in a line with two pursuers and one evader. Dyn. Games Appl. **2**(2), 228–257 (2012)
7. Garcia, E., Casbeer, D.W., Fuchs, Z.E., Pachter, M.: Aircraft defense differential game with non-zero capture radius. In: 20th IFAC World Congress (2017)
8. Garcia, E., Casbeer, D.W., Pachter, M.: Active target defense differential game with fast defender. In: American Control Conference, pp. 3752–3757 (2015)
9. Garcia, E., Casbeer, D.W., Pachter, M.: Cooperative strategies for optimal aircraft defense from an attacking missile. J. Guid. Control. Dyn. **38**(8), 1510–1520 (2015)
10. Garcia, E., Casbeer, D.W., Pachter, M.: Escape regions of the active target defense differential game. In: ASME Dynamic Systems and Control Conference (2015)
11. Garcia, E., Casbeer, D.W., Pham, K., Pachter, M.: Cooperative aircraft defense from an attacking missile. In: 53rd IEEE Conference on Decision and Control, pp. 2926–2931 (2014)
12. Garcia, E., Casbeer, D.W., Pham, K., Pachter, M.: Cooperative aircraft defense from an attacking missile using proportional navigation. In: AIAA Guidence, Navigation, and Control Conference (2015)
13. Huang, H., Zhang, W., Ding, J., Stipanovic, D.M., Tomlin, C.J.: Guaranteed decentralized pursuit-evasion in the plane with multiple pursuers. In: 50th IEEE Conference on Decision and Control and European Control Conference, pp. 4835–4840 (2011)
14. Isaacs, R.: Differential Games. Wiley, New York (1965)
15. Pachter, M., Garcia, E., Casbeer, D.W.: Active target defense differential game. In: 52nd Annual Allerton Conference on Communication, Control, and Computing, pp. 46–53 (2014)
16. Perelman, A., Shima, T., Rusnak, I.: Cooperative differential games strategies for active aircraft protection from a homing missile. J. Guid. Control. Dyn. **34**(3), 761–773 (2011)
17. Pham, K.: Risk-averse based paradigms for uncertainty forecast and management in differential games of persistent disruptions and denials. In: American Control Conference, pp. 842–849 (2010)
18. Prokopov, O., Shima, T.: Linear quadratic optimal cooperative strategies for active aircraft protection. J. Guid. Control. Dyn. **36**(3), 753–764 (2013)
19. Ratnoo, A., Shima, T.: Line-of-sight interceptor guidance for defending an aircraft. J. Guid. Control. Dyn. **34**(2), 522–532 (2011)
20. Ratnoo, A., Shima, T.: Guidance strategies against defended aerial targets. J. Guid. Control. Dyn. **35**(4), 1059–1068 (2012)
21. Rubinsky, S., Gutman, S.: Three body guaranteed pursuit and evasion. In: AIAA Guidance, Navigation, and Control Conference, pp. 1–24 (2012)
22. Rubinsky, S., Gutman, S.: Three-player pursuit and evasion conflict. J. Guid. Control. Dyn. **37**(1), 98–110 (2014)
23. Rusnak, I.: The lady, the bandits, and the bodyguards–a two team dynamic game. In: 16th IFAC World Congress, pp. 441–446 (2005)
24. Rusnak, I., Weiss, H., Hexner, G.: Guidance laws in target-missile-defender scenario with an aggressive defender. In: 18th IFAC World Congress, pp. 9349–9354 (2011)
25. Scott, W., Leonard, N.E.: Pursuit, herding and evasion: a three-agent model of caribou predation. In: American Control Conference, pp. 2978–2983 (2013)
26. Shaferman, V., Shima, T.: Cooperative multiple-model adaptive guidance for an aircraft defending missile. J. Guid. Control. Dyn. **33**(6), 1801–1813 (2010)
27. Shima, T.: Optimal cooperative pursuit and evasion strategies against a homing missile. J. Guid. Control. Dyn. **34**(2), 414–425 (2011)
28. Yamasaki, T., Balakrishnan, S.N.: Triangle intercept guidance for aerial defense. In: AIAA Guidance, Navigation, and Control Conference. American Institute of Aeronautics and Astronautics (2010)
29. Yamasaki, T., Balakrishnan, S.N., Takano, H.: Modified command to line-of-sight intercept guidance for aircraft defense. J. Guid. Control. Dyn. **36**(3), 898–902 (2013)

Dr. David W. Casbeer is the tech area lead for the UAV Cooperative and Intelligent Control Team within the Control Science Center of Excellence in the Air Force Research Laboratory's Aerospace Systems Directorate. The UAV team focuses on decision making, planning, and coordination for multiple autonomous UAVs acting and reacting in uncertain and adversarial environments. Dr. Casbeer received the BS and PhD degrees from Brigham Young University in 2003 and 2009, respectively, where he advanced theory describing the statistics of decentralized estimation techniques. In 2016, Dr. Casbeer was awarded AFRL's Early Career Award for distinguished foundational research in multi-agent control. He currently serves as the chair for the AIAA Intelligent Systems Technical Committee and as a Senior Editor for the Journal of Intelligent and Robotic Systems.

Eloy Garcia received the Ph.D. degree from the Electrical Engineering Department, University of Notre Dame, Notre Dame, IN, in 2012. He also holds M.S. degrees from the University of Illinois at Chicago, Chicago, IL, and the University of Notre Dame, Notre Dame, IN, both in electrical engineering. From 2012 to 2016, he was a Research Scientist with Infoscitex Corporation, Dayton, OH. He is currently a Research Engineer with the Control Science Center of Excellence, Air Force Research Laboratory, Wright-Patterson Air Force Base, OH. He is author/editor of the books Model-based Control of Networked Systems and Cooperative Control of Multi-agent Systems: Theory and Applications. His current research interests include cooperative control of multi-agent systems, optimal and cooperative missile guidance, and differential games.

Dr. Meir Pachter is a Professor of Electrical Engineering at the Air Force Institute of Technology, Wright-Patterson AFB.

Dr. Pachter received the BS and MS degrees in Aerospace Engineering in 1967 and 1969, respectively, and the Ph.D. degree in Applied Mathematics in 1975, all from the Israel Institute of Technology.

Dr. Pachter held research and teaching positions at the Israel Institute of Technology, the Council for Scientific and Industrial Research in South Africa, Virginia Polytechnic Institute, Harvard University and Integrated Systems, Inc.

Dr. Pachter is interested in the application of mathematics to the solution of engineering and scientific problems. His current areas of interest include military operations optimization, dynamic games, cooperative control, estimation and optimization, statistical signal processing, adaptive optics, inertial navigation, and GPS navigation. For his work on adaptive and reconfigurable flight control he received the AF Air Vehicle's Directorate Foulois award for 1994, together with Phil Chandler and Mark Mears.

Dr. Pachter is a Fellow of the IEEE.